



Research Article

Dynamics of circulating lymphocytes responding to human experimental enterotoxigenic *Escherichia coli* infection

Sehee Rim^{#1} , Sunniva T. Sakkestad¹, Fan Zhou¹, Stein-Erik Gullaksen^{2,3}, Jørn Skavland¹, Sudhir K. Chauhan⁴, Hans Steinsland^{5,6} and Kurt Hanevik^{1,7} 

1st
time

author

Read more about EJI's
first-time authors

¹ Department of Clinical Science, Faculty of Medicine, University of Bergen, Bergen, Norway

² Department of Clinical Science, Centre of Cancer Biomarkers (CCBIO), University of Bergen, Bergen, Norway

³ Hematology Section, Department of Internal Medicine, Helse Bergen, Bergen, Norway

⁴ Division of Cancer Medicine, Department of Cancer Immunology, Oslo University Hospital, Oslo, Norway

⁵ Department of Global Public Health and Primary Care, Faculty of Medicine, Centre for Intervention Science in Maternal and Child Health (CISMAC), Centre for International Health, University of Bergen, Bergen, Norway

⁶ Department of Biomedicine, Faculty of Medicine, University of Bergen, Bergen, Norway

⁷ Department of Medicine, Norwegian National Advisory Unit on Tropical Infectious Diseases, Haukeland University Hospital, Bergen, Norway

Enterotoxigenic *Escherichia coli* (ETEC) is an important cause of children's and travelers' diarrhea, with no licensed vaccine. This study aimed to explore the role of cellular immunity in protection against human ETEC infection. Nine volunteers were experimentally infected with ETEC, of which six developed diarrhea. Lymphocytes were collected from peripheral blood buffy coats, before and 3, 5, 6, 7, 10, and 28 days after dose ingestion, and 34 phenotypic and functional markers were examined by mass cytometry. Thirty-three cell populations, derived by manually merging 139 cell clusters from the X-shift unsupervised clustering algorithm, were analyzed. Initially, the diarrhea group responded with increased CD56dim CD16⁺ natural killer cells, dendritic cells tended to rise, and mucosal-associated invariant T cells decreased. On day 5-7, an increase in plasmablasts was paralleled by a consistent rise in CD4⁺ Th17-like effector memory and regulatory cell subsets. CD4⁺ Th17-like central memory cells peaked on day 10. All Th17-like cell populations showed increased expression of activation, gut-homing, and proliferation markers. Interestingly, in the nondiarrhea group, these same CD4⁺ Th17-like cell populations expanded earlier, normalizing around day 7. Earlier development of these CD4⁺ Th17-like cell populations in the nondiarrhea group may suggest a recall response and a potential role in controlling ETEC infections.

Keywords: CD57 · CyTOF · longitudinal · mucosal immunity · TW10722



Additional supporting information may be found online in the Supporting Information section at the end of the article.

Correspondence: Prof. Kurt Hanevik
e-mail: kurt.hanevik@uib.no

[#]First-time first author: Sehee Rim

Introduction

Infection with enterotoxigenic *Escherichia coli* (ETEC) is an important cause of diarrheal disease in low-and-middle income countries (LMICs), causing around 75 million diarrheal episodes and 50,000 deaths yearly, mostly in travelers and in children under the age of 5 years [1]{Khalil, 2018 #1232}. Although considerable efforts have been made to develop vaccines that may protect against ETEC diarrhea, there is no available licensed vaccine [2]{Bourgeois, 2016 #1066}.

After ingestion, ETEC colonizes the human small intestinal mucosa and cause diarrheal disease by secreting one or both of two enterotoxins called heat-labile toxin and heat-stable toxin, leading to diarrhea through the secretion of ions and subsequent osmotic water loss [3]. Since ETEC is a noninvasive pathogen, immunoprotection against ETEC is believed to be conferred primarily by neutralizing IgA antibodies secreted into the gut lumen, and most ETEC vaccine development efforts have therefore been focused on eliciting humoral immune responses [4].

Along with humoral responses, it has been hypothesized that several immune cell subsets contributes to tissue integrity, pathogen clearance, and protection [5, 6], limiting bacterial pathogens at mucosal sites [7]. An important interplay between natural killer (NK) cells and dendritic cells (DC) in bacterial infection has also been shown [8].

It is suggested that cells of the innate and adaptive immune systems contribute to protection against ETEC infection, as well as to modulation of immunological memory [9, 10]. Long-lasting antigen-specific CD4⁺ T-cell responses following ETEC infections have been reported [11, 12]. A role for cellular immunity may include indirectly helping B cells to produce high-affinity ETEC-specific antibodies [13, 14], and by directly enhancing intestinal epithelium anti-microbial peptide production and IgA transport [7]. Relatively recently, the cytokine IL-17 has been found to be associated with extracellular bacterial infections [15, 16]. IL-17 producing T cells, named as Th17 cells, were found and characterized by Annunziato et al. at several sites, including the small intestine of patients with Crohn's disease [17]. Effector and memory Th17 cells are especially capable of strong IL-17 production only a few hours after antigenic stimulation [18]. The role of different lymphocyte subsets, as well as potential correlates of protection for ETEC infection, needs to be further elucidated.

With the availability of mass cytometry technology, allowing single-cell mass spectrometry-based quantitation of cell-bound antibody markers, it is possible to design multiplex assays for quantitating a high number of cell surface antigens [19]. The use of mass cytometry in *Salmonella* infection identified a distinct activated CD4⁺ T effector cell subset hypothesized to play an important role in protection against re-infection [20] and showed how T regulatory cells may modulate disease outcomes [21].

To further explore the dynamics of cell-mediated immune responses to ETEC infections, we used mass cytometry to characterize phenotypes and dynamics in the circulating PBL populations following experimental infections with WT ETEC strain TW10722.

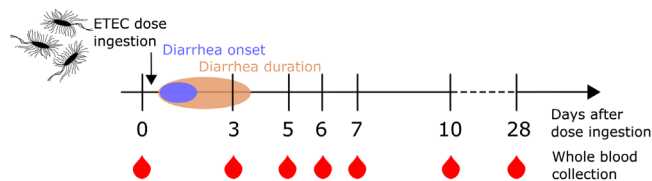


Figure 1. Timeline showing the main events during experimental TW10722 infection. A total of nine volunteers administered ETEC dose on day 0 and blood samples for mass cytometry were taken before and after days 0, 3, 5, 6, 7, and 28 after dose ingestion. Median diarrhea onset was 24 h after dose ingestion, lasting for 3 days.

Results

Study setting and volunteers

Of the nine volunteers enrolled in the study (median age 22 years (range 20–23 years), eight females, one male), six (67%) developed diarrhea of varying severity within the second day after the infection, while three (33%) did not (Supporting Information Table S3). All volunteers were confirmed to be ETEC infected by positive daily stool samples as previously reported [12]. Development of diarrhea was associated with ETEC colonization levels with a maximum ETEC DNA percentage of 0.6% or below in the nondiarrhea group and ranged between 1% and 11% in the diarrhea group [22]. No volunteers developed fever (temperature >38°C). Main events during the ETEC experimental infection are shown in Fig. 1. A total of 33 lymphocyte populations were obtained for further analysis, as shown in Table 1. Dynamics of the proportion of each population, presented as median baseline values on day 0 and fold changes at each time point afterwards, are shown in Fig. 2.

Innate immunity: rising DCs and NK cells, decreased MAIT cells in diarrhea group

Cell populations 01–12 in Table 1 represent innate immune cells. Baseline proportions of conventional DC and plasmacytoid DC did not differ between the diarrhea and nondiarrhea groups. Both conventional DC and plasmacytoid DC tended to increase in proportion in the early phase of the infection (day 3) in both groups, although not significantly (Fig. 2).

CD56^{dim} CD16⁺ NK cells increased 1.6-fold from day 0 to 3 and stayed elevated in the diarrhea group, in which the population also exhibited an elevated $\beta 7$ expression (supplementary chart [SC]-S04). CD4⁺ NKT cells had similar baseline proportions in both groups and did not change significantly (Fig. 2). However, we observed CD95 and inducible T-cell co-stimulator (ICOS) upregulation in the diarrhea group during days 3 to 6 (SC-S04).

In the diarrhea group, both the CD8⁺ and the CD4⁺ CD8⁻ mucosal associated invariant T (MAIT) cell population was reduced to half its proportion by day 3, and the populations continued to be reduced in comparison with baseline throughout the

Table 1. Cell clusters obtained from the semi-supervised cell clustering and their nomenclature based on the marker expression. The column "No" denotes a number given to the population.

		Cell clusters	No.	Marker expression
Dendritic cells		Conventional DC (cDC)	01	CD11c ⁺ Lin neg [*] HLA-DR ⁺
		Plasmacytoid DC (pDC)	02	CD123 ⁺ Lin neg [*] HLA-DR ⁺
Natural killer (NK) cells		CD56 ^{bright} CD16 ⁻	03	CD56 ⁺⁺ CD16 ⁻ CD3 ⁻
		CD56 ^{dim} CD16 ⁺	04	CD56 ⁺ CD16 ⁺ CD3 ⁻
Natural killer T (NKT) cells		CD4 ⁺ NKT	05	CD3 ⁺ CD56 ⁺ CD4 ⁺ CD8 ^{dim}
		NKT other	06	CD3 ⁺ CD56 ⁺
Mucosal associated invariant T (MAIT) cells		CD8 ⁺ MAIT	07	CD3 ⁺ TCR V α 7.2 ⁺ CD161 ⁺ CD8 ⁺
		NKT-like MAIT	08	CD3 ⁺ TCR V α 7.2 ⁺ CD161 ⁺ CD56 ⁺
		CD4 ⁻ CD8 ⁻ MAIT	09	CD3 ⁺ TCR V α 7.2 ⁺ CD161 ⁺ CD4 ⁻ CD8 ⁻
Gamma-delta ($\gamma\delta$) T cells		CD8 ⁺ $\gamma\delta$ T	10	CD3 ⁺ TCR $\gamma\delta$ ⁺ CD8 ⁺
		NKT-like $\gamma\delta$ T	11	CD3 ⁺ TCR $\gamma\delta$ ⁺ CD56 ⁺
		CD4 ⁻ CD8 ⁻ $\gamma\delta$ T	12	CD3 ⁺ TCR $\gamma\delta$ ⁺ CD4 ⁻ CD8 ⁻
CD4 ⁺ T cells	Naive	Naive	13	CD3 ⁺ CD4 ⁺ CD45RO ⁻ CD27 ⁺ CD127 ⁺
		Naive CD127 ⁻	14	CD3 ⁺ CD4 ⁺ CD45RO ⁻ CD27 ⁺ CD127 ⁻
		Natural regulatory	15	CD3 ⁺ CD4 ⁺ CD45RO ⁻ CD25 ⁺ CD127 ⁻
	Effector memory (EM)	Effector memory	16	CD3 ⁺ CD4 ⁺ CD45RO ⁺ CD27 ⁻
		T _{EMRA} CD127 ⁺	17	CD3 ⁺ CD4 ⁺ CD45RO ⁻ CD27 ⁻ CD127 ⁺
		T _{EMRA} CD127 ⁻	18	CD3 ⁺ CD4 ⁺ CD45RO ⁻ CD27 ⁻ CD127 ⁻
		Th17-like effector memory (Th17-like EM)	19	CD3 ⁺ CD4 ⁺ CD45RO ⁺ CD27 ⁻ CD39 ⁺ CD161 ⁺
		Effector memory regulatory	20	CD3 ⁺ CD4 ⁺ CD45RO ⁺ CD27 ⁻ CD25 ⁺ CD127 ⁻
	Central Memory (CM)	Th17-like effector memory regulatory (Th17-like EM reg)	21	CD3 ⁺ CD4 ⁺ CD45RO ⁺ CD27 ⁻ CD25 ⁺ CD127 ⁻ CD39 ⁺ CD161 ⁺
		Central memory	22	CD3 ⁺ CD4 ⁺ CD45RO ⁺ CD27 ⁺
		Th17-like central memory (Th17-like CM)	23	CD3 ⁺ CD4 ⁺ CD45RO ⁺ CD27 ⁺ CD39 ⁺ CD161 ⁺
		Central memory regulatory (Th17-like CM reg)	24	CD3 ⁺ CD4 ⁺ CD45RO ⁺ CD27 ⁺ CD25 ⁺ CD127 ⁻
CD8 ⁺ T cells	Naive	25	CD3 ⁺ CD8 ⁺ CD45RO ⁻ CD27 ⁺ CD127 ⁺	
	Naive CD127 ⁻	26	CD3 ⁺ CD8 ⁺ CD45RO ⁻ CD27 ⁺ CD127 ⁻	
	Effector memory	27	CD3 ⁺ CD8 ⁺ CD45RO ⁺ CD27 ⁻	
	T _{EMRA} CD127 ⁺	28	CD3 ⁺ CD8 ⁺ CD45RO ⁻ CD27 ⁻ CD127 ⁺	
	T _{EMRA} CD127 ⁻	29	CD3 ⁺ CD8 ⁺ CD45RO ⁻ CD27 ⁻ CD127 ⁻	
	Central memory	30	CD3 ⁺ CD8 ⁺ CD45RO ⁺ CD27 ⁺	
B cells	Naive	31	CD19 ⁺ CD20 ⁺ IgD ⁺ CD27 ⁻ CD38 ⁺ CD24 ⁺	
	Plasmablast	32	CD19 ⁺ CD20 ⁻ CD27 ⁺ CD38 ⁺ CD39 ⁺	
	Memory	33	CD19 ⁺ CD20 ⁺ CD11c ⁺ CD39 ⁺ IgD ⁻	

* Lin neg = Lineage markers (CD56, CD19, CD20, CD3) negative.

follow-up. An early onset increase in the expression of HLA-DR, CD95, and ICOS in all three MAIT cell subpopulations was noted in the diarrhea group, most markedly on day 3 and 5 (SC-S07-S09).

The three $\gamma\delta$ T-cell populations remained relatively stable except for a rise on day 10 in the NKT-like $\gamma\delta$ T-cell subpopulation (Fig. 2). The diarrhea group showed an increased HLA-DR expression at day 5 across $\gamma\delta$ populations and a modestly increased early expression of CD38 and ICOS in the CD8⁺ and the CD4⁻ CD8⁻ $\gamma\delta$ populations (SC-S10-S12). In the CD8⁺ $\gamma\delta$ T-cell subpopulation, as well as the two NKT populations, CD57 increased during and

after infection in the diarrhea group as opposed to a decreased CD57 expression in the nondiarrhea group (SC-S05-S06, S10).

T cells: Less naïve CD127⁻ CD4 T cells and Tregs in the diarrhea group at baseline

Naïve T-cell clusters identified by the unsupervised algorithm were divided largely by their expression of CD127 (Table 1). CD4⁺ naïve T cells seemed less abundant at baseline in the diarrhea group compared to the nondiarrhea group, with much of

Proportion before Infection and Fold Changes of Cell Populations

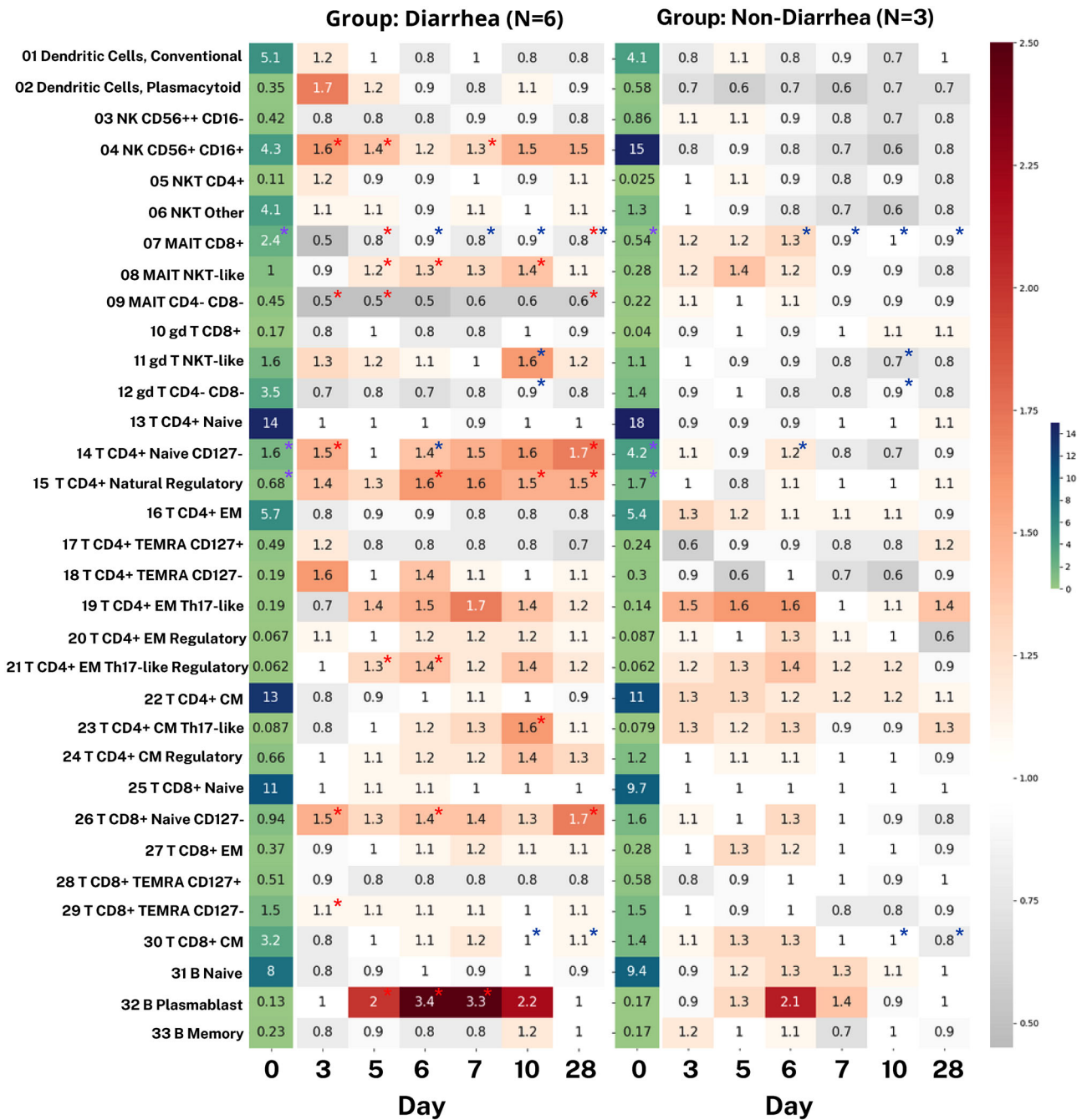


Figure 2. Heatmap showing baseline (pre-infection) cell population proportions and fold changes from baseline at several timepoints after ETEC infection in the diarrhea and nondiarrhea group. Numbers in the “day 0”-column represent the baseline cell population as a median percentage (%) of the total peripheral blood lymphocyte population. Numbers in the “day 3” to “day 28” columns represent medians of fold changes calculated by dividing cell population proportion for each timepoint by the baseline value for each volunteer. Red asterisks denote a significant fold-change from baseline within the group (p -value < 0.05 , Wilcoxon signed ranked test). Purple asterisks denote a significant difference in baseline levels between the diarrhea and nondiarrhea groups (p -value < 0.05 , Mann-Whitney U test). Blue asterisks denote a significant difference in fold-change between the diarrhea and nondiarrhea groups (p -value < 0.05 , Mann-Whitney U test).

the difference being due to less naïve CD127⁻ CD4 T cells (1.6% vs. 4.2%) (Fig. 2). In both CD4 and CD8 compartments, there were similar small, sustained increases in these naïve CD127⁻ populations following the infection (Fig. 2). In all four naïve

T-cell subsets, there were modest upregulations of the HLA-DR, ICOS, and $\beta 7$ expression (SC-13-14 and 25-26).

Baseline natural regulatory T cells (Tregs) were significantly more abundant in the nondiarrhea group (1.7%) than in the

diarrhea group (0.68%). While Treg levels remained stable in the nondiarrhea group, they increased significantly in the diarrhea group with peak levels obtained on day 6. Also, HLA-DR seemed more strongly expressed in Tregs from day 3 in the diarrhea group (SC-15). The same pattern of increased levels in the diarrhea group was noted for central memory regulatory T cells, however, peak levels were achieved on day 10, and the population seemed to have a more broad upregulation of activation markers CD38, CD71, HLA-DR, ICOS, and PD-1 from day 3 lasting until day 28 (SC-24).

Antigen experienced T cells can be divided into effector memory T (T_{EM}) cells, central memory T (T_{CM}) cells [23], and effector memory T cells re-expressing CD45RA (T_{EMRA}) [24]. These populations had similar baseline proportions in both groups. Interestingly, T_{EM} and T_{CM} remained relatively unchanged in the diarrhea group, while there seemed to be a modest early rise in the nondiarrhea group (Fig. 2). However, T_{EM} populations in the diarrhea group displayed an early rise in the expression of HLA-DR, ICOS, PD-1, and CD24 from day 3 lasting until day 28.

In the CD8 compartment, most subpopulations remained relatively unchanged for a modest rise in the CD127- T_{EMRA} cell population in the diarrhea group (Fig. 2, SC-18 and 29). Central memory regulatory T cells tended to gradually increase, peaking on day 10 in the diarrhea group, with a broad and moderate upregulation of CD38, CD71, HLA-DR, ICOS, and PD-1 from day 3 persisting to day 28 (SC-24).

Th17-like CD4 T cells: Increase in the diarrhea group, earlier increase in the nondiarrhea group

CD161 was shown already in 2008 to be a surface marker of IL-17-producing T cells [25] and co-expression of CD161 and CD39 in CD4 T cells was later shown to be further distinctive of Th17 cells [26]. The applied unsupervised algorithm identified several such Th17-like populations in the present study, and the changes seen in the CD4⁺ T-cell populations were accentuated in the Th17-like cell populations. Th17-like EM cell proportions increased gradually after the infection in both groups, but they peaked sooner in the nondiarrhea group (day 3) compared to the diarrhea group (day 7) (Fig. 3A). In the diarrhea group, the proliferation marker CD71 expression seemed to increase on day 5 and 6, together with increased expression of ICOS, PD-1, and β 7 on days 5–10. In the nondiarrhea group, the activation marker expression was less pronounced, and PD-1 expression seemed to decrease rather than increase after infection.

Th17-like EM regulatory T cells increased 1.3-fold at day 5 and 6 in both groups, although an earlier and more short-lasting response was observed in the nondiarrhea group. In the diarrhea group, we observed increased CD71, ICOS, and β 7 expression on day 5–6, followed by a decrease afterward (Fig. 3B). Interestingly, HLA-DR expression in this population tended to decrease in both groups, along with decreased PD-1 expression the nondiarrhea group.

The small Th17-like T_{CM} cell population showed no baseline differences. However, following infection the population increased early (day 3) in the nondiarrhea group as compared to late (day 10) in the diarrhea group (Figs. 2 and 3C). Also, in the diarrhea group, functional markers including CD71, ICOS, PD-1, and β 7 showed a gradual increase in expression from day 3 and lasting until day 28. This response was barely seen in the nondiarrhea group.

B cells: Increased plasmablasts correlating with Th17-like T_{CM} cells

The plasmablast proportion increased 3.5-fold (peak on day 7) in the diarrhea group and 2.1-fold (peak on day 6) in the nondiarrhea group. Expression of HLA-DR and CD71 peaked on day 5 after the infection, while IgA and integrin β 7 expression was most pronounced 6–10 days after infection (Fig. 3D).

We found no clear differences in baseline levels in any of the other three B-cell subpopulations. Naïve B cells tended to increase 1.3-fold from day 0 to day 6 and 7 in the nondiarrhea group (Fig. 2), and showed minor increases in expression of CD24, IgA, and β 7 in the diarrhea group.

Interestingly, the proportions of Th17-like T_{CM} cells on day 10 correlated with the proportions of plasmablasts on day 6 ($p = 0.006$, $r = 0.81$) and day 7 ($p = 0.008$, $r = 0.68$) ($n = 9$). Proportions of plasmablasts on day 6 had significant correlations with those of Th17-like T_{EM} cells on days 5, 6, 7, 10, and 28 ($p = 0.03$ or lower) (Supporting Information Fig. S1).

Discussion and conclusion

In this study, we characterized the dynamics of immune cell populations in nine volunteers experimentally infected with ETEC using mass cytometry. In the analyses, we focused on changes in proportions and expression of functional markers in circulating lymphocytes and identified highly interesting differences among volunteers who developed diarrhea compared to those who did not.

Early innate responses were noticed in the diarrhea group. The data presented here indicate a role for innate immune responses in ETEC infection, which may be important players for modulating the adaptive immune response. For example, the increased proportion and gut-homing of CD56^{dim} CD16⁺ NK cells after infection in the diarrhea group indicates a role even in a noninvasive infection like ETEC. It may reflect an inflammatory response in the early phase, and later a potential drive to repair damaged mucosa [27].

NKTs can be activated indirectly by cytokines secreted from antigen-presenting cells (APCs) following recognition of microbial molecules by their TLRs, but also directly by recognizing glycolipid antigens presented by the MHC class I-related glycoprotein CD1d on various cells [28]. ICOS, a costimulatory molecule required for the survival and homeostasis of NKT cells,

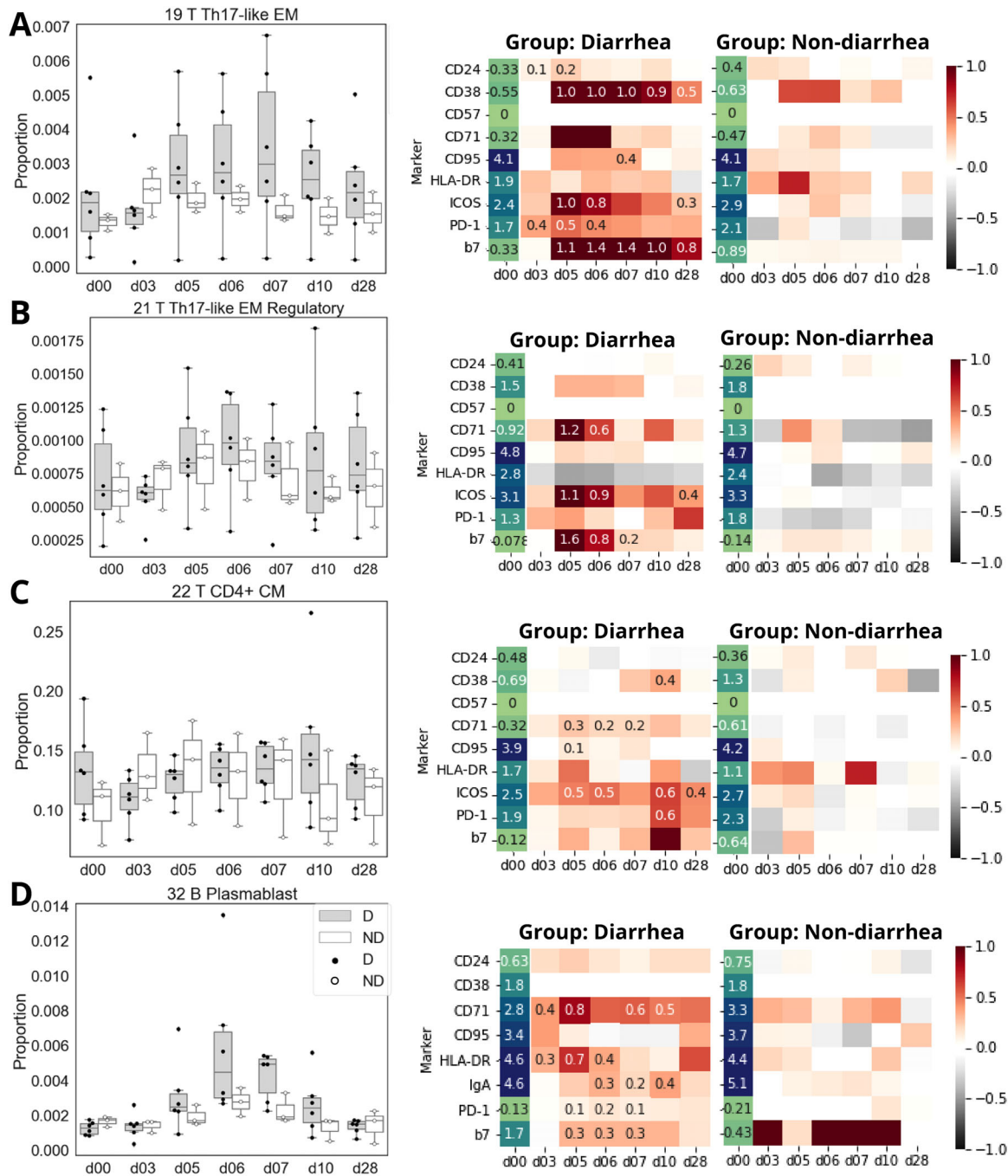


Figure 3. Boxplots on the left side display the proportions of Th17-like EM cells; Th17-like EM regulatory cells; Th17-like CM cells and plasmablasts for the diarrhea group (gray, $n = 6$) and the nondiarrhea group (white, $n = 3$). Heatmaps on the right side display the signal intensity of selected functional cell surface markers. The signal intensity is given as arcsinh-transformed 80th percentiles for each marker at day 0 (baseline) and the change from this baseline value at days 3, 5, 6, 7, 10, and 28 after infection. Further explanation is found in the Supporting Information. Significant arcsinh-transformed 80th percentile values are marked with their values of difference present in the heatmap ($p < 0.05$, Wilcoxon signed rank test). Testing was not performed for the nondiarrhea group due to few volunteers in this group.

was found to be upregulated in NKT cells in the diarrhea group, suggesting activation of NKT cell subpopulations could be a part of the innate immune response against ETEC.

Escherichia coli produces phosphoantigens, such as 3-formyl-1-butyl-pyrophosphate and TUBag2, which are both potent

activators for $\gamma\delta$ T cells [29, 30]. A previous study of parenteral vaccination against enterohemorrhagic *Escherichia coli* in cattle $\gamma\delta$ T cells maintained a proinflammatory environment in the gut mucosa by recruiting lymphocytes and producing IFN- γ , IL-4, and IL-10, with detectable cytokine levels up until 6 weeks after

vaccination [31]. Long-lasting increases of CD57, ICOS, HLA-DR in $\gamma\delta$ T cells were observed in $\gamma\delta$ T cells in the present study, suggesting a role for $\gamma\delta$ T cells in maintaining a proinflammatory environment.

Increased expression of activation marker CD38, proliferation marker Ki-67, and gut-homing markers $\beta 7$ and CCR9 in MAIT cells, but no change in overall frequency, has been observed 7 days after ETEC infection [32]. Our study adds granularity to that finding by including earlier timepoints to the study of MAIT cell dynamics, showing a tendency for decreased proportions of all MAIT cell subpopulations in the diarrhea group at day 3 (Fig. 2). In a previous study, MAIT cells were found in lungs, with a corresponding reduction in the circulation, shortly after infection with *Mycobacterium tuberculosis* [33]. MAIT cell reduction was also observed in a *Salmonella enterica* serovar Typhi human challenge study in which peripheral CD8⁺ MAIT cells declined sharply 2–3 days following infection in volunteers who later developed typhoid disease [34]. Also, these CD8⁺ MAIT cells exhibited upregulation of activation and homing markers for intestines and damaged tissues [34]. During the infection phase, MAIT cells are known to participate in the lysis of infected cells for limiting the bacterial spread to the organism [33].

Although there were little changes in typical naïve CD4 and CD8 T cells, the sustained increase in the CD127⁻ naïve T-cell subpopulations are likely to be circulating T cells, which recently exit from secondary lymphoid organs [35] and may therefore reflect a generally increased lymphocyte mobilization induced by the infection.

During gut mucosal infections, the homeostasis of the gut milieu is disrupted. There is normally a balance maintained by regulatory T cells and Th17 cells with low affinity against specific microbes [36]. CD4⁺ Th cells of the Th17 lineage are believed to play important roles in the defense against pathogens at mucosal barriers, for example, by inducing polymeric immunoglobulin receptor facilitating IgA delivery to the intestinal lumen and by stimulating production of antimicrobial defensins [7, 37] {Khader, 2009 #1291}. Several studies in mice indicate that Th17 cells are induced and produce IL-17 to attract neutrophils and monocytes, after infection with *E. coli*, and several other gut pathogens such as *Salmonella*, *Pseudomonas* and *Bordetella* [38, 39].

In addition to producing IL-17, Th17 cells have also been shown to produce other cytokines promoting intestinal inflammation and mediating direct bacteria toxicity at mucosal membranes [40]. An IL-17-dominated systemic and mucosal immune response has been shown after immunization with ETEC antigens in a pig model [41], and trials of an oral inactivated ETEC vaccine candidate elicited gut homing follicular Th17 helper cells [14].

In the present study, the increased proportions of Th17-like T_{EM}, Th17-like T_{EM} regulatory cells, and Th17-like T_{CM} in both the diarrhea and nondiarrhea groups support previous findings on responsiveness of Th17-populations in adaptive and specific immunity against ETEC in humans. The dynamics of Th17-like T_{CM} in the diarrhea group, peaking at day 10 with pronounced expression of CD71, ICOS, and PD-1, and its correlation with cir-

culating plasmablasts may suggest a recirculation of this population to target tissues or BM for establishment of long-lasting memory.

In the only other published trial to date using mass cytometry to study immunological outcomes following ETEC infection, McArthur et al. examined six healthy adult volunteers infected with the H10407 strain [13], and found higher levels of ETEC antigen responsive gut-homing CD4⁺ T cells at baseline, and at day 3, in three volunteers developing mild or no diarrhea. This parallels our finding of an early rise in several gut-homing Th17-like cell populations at day 3 in the nondiarrhea group, and we also provide data for similar populations appearing some days later in volunteers developing diarrhea.

The observation of early responsive CD4⁺ T-cell populations in the nondiarrhea group indicates a role for these populations in immunological resilience against infection. A significantly higher proportion of natural CD4⁺ T regulatory cells in the nondiarrhea group at baseline suggests they contribute in mediating immunological resilience in the initial phase, potentially limiting the inflammatory response [42]. Likewise, the earlier temporary rise in proportion and activation of circulating CD4 T EM and CM cell populations (most distinctly seen in the Th17-like compartments on day 3–5) in the nondiarrhea group indicates a rapid adaptive effector response in these volunteers. Previously, we have reported an expansion of activated antigen-specific CD4 T cells (CD134⁺ CD25⁺) using flow cytometry in fresh PBMC samples at day 10 from volunteers in this study. We also found increases in IgA and IgG antibody levels against ETEC-specific antigens such as CS5 (where CS is coli surface antigens), CS6, and YghJ at days 10 and 28 [12].

Several studies have reported an increase in circulating plasmablasts around 5–7 days after inoculation as an important measure of the specific B-cell response to ETEC infection responsible for establishing and distributing plasma cells along gut-associated mucosa [14, 43]. In the present study, we observed an increased proportion of plasmablasts with increased expression of proliferation marker CD71 as well as IgA and HLA-DR at days 6 and 7, which corresponds with previous studies of plasmablast dynamics.

This study has several limitations. It included few volunteers and was designed to be an exploratory study, providing high-resolution data for further research. We present findings with related arguments along with *p*-values, such as consistent fold-change over several days, and immunologically coherent responses to compensate for the small sample size. Further studies are needed to obtain more robust estimates, preferably including an internal counting standard so that changes in absolute cell counts can also be assessed.

Volunteers that were recruited to this study were mostly females. Immune responses in this study may therefore not be reflected in both sexes. Also, we cannot fully ascertain previous exposure or nonexposure of volunteers to ETEC.

Some caution is warranted in interpreting the change in populations of CD56^{dim} CD16⁺ NK cells and CD4⁺ natural regulatory cells, as they are presenting with nondynamic, persistently higher

proportions than in the baseline in the diarrhea group. Potentially, the higher postbaseline levels here are due to a falsely low baseline.

Regrettably, although we put much effort into identifying an antibody clone and a staining method for the chemokine receptor CXCR5 that would work with our fixed lymphocyte samples, we did not achieve adequate staining of T cells, barring detection of circulating T follicular helper cells.

The antibiotic treatment administered to the volunteers at day 5, or before, did not seem to affect immune cell frequencies and dynamics much as no distinct shift in populations were seen in the volunteers at the time they received the antibiotics. However, antibiotic treatment in the diarrhea group on day 2 or 3 possibly limited the natural course of infection and exposure to ETEC, resulting in a weaker and/or shorter immune response.

Using fixed cells limited our possibility to stimulate cells for ETEC-specific antigens and evaluate cytokine expression. Due to this, we could not directly determine whether the identified Th17-like populations produce IL-17 or perhaps also co-express IFN- γ [44]. This study presents an analysis based on phenotypic surface markers and their fold changes in proportions, which potentially is a generic peripheral lymphocyte response during ETEC infection. Assessment of its specificity for ETEC will need future characterization by in-depth analysis of functional markers in live cells. However, previously published ETEC antigen-specific T-cell responses at day 10 after infection by our group [12, 45] corroborate specificity of T-cell findings in the present study.

Since the present study sought to explore all major lymphocyte subsets, the panel had limited capacity for subtyping some cell populations. For example, for dendritic cells, we used only major markers (e.g., CD123, CD11c, and HLA-DR), which precluded detailed characterization.

Natural ETEC infection is known to protect against homologous ETEC challenge [46]. The lymphocyte subsets responding to natural ETEC infection explored in the present study may be important in the development of that protection. This can be further tested in larger studies designed for in-depth and specific analysis, at the timepoints where they appear altered. Studies to evaluate the ability of vaccine candidates and formulations to elicit beneficial specific cellular immune responses could be valuable to guide vaccine development against infant diarrheal diseases. Recent innovations in small volume, whole blood sample staining, and preservation methods will facilitate such studies in low-and-middle income country infants [47–49].

To conclude, in this exploratory study of human lymphocyte responses to experimental ETEC infection, we observed early changes in the proportions of innate immune cell populations such as temporary decreases, especially in CD8⁺ MAIT cells, as well as increased activation markers in all MAIT cell populations in volunteers developing diarrhea. From day 5, Th17-like EM cell populations were observed to rise, followed by plasmablasts and Th17-like CM cells in the diarrhea group. Interestingly, in volunteers who did not develop diarrhea, the MAIT cell decrease was not seen, and responsive Th17-like cell populations were seen ele-

vated already at day 3. These differences in Th17-like cell population kinetics may reflect a protective cellular recall response, which could contribute to resilience against symptomatic ETEC infection in volunteers not developing diarrhea.

Materials and methods

Study setting and volunteers

The experimental infections took place at Haukeland University Hospital, Bergen, Norway, in the period 2014 to 2018 [12]. We focused our current study on nine volunteers enrolled during winter 2017–2018 who ingested doses of 1×10^9 or 1×10^{10} colony-forming units (CFUs) (Supporting Information Table S3) of ETEC strain TW10722 (serotype O115:H5), which belongs to an ETEC family associated with childhood diarrhea [12, 50] and produces heat-stable toxin. Volunteers had not visited ETEC-endemic countries during the last 12 months before entering the study. After dose ingestion, volunteers stayed in a hospital wardroom, being closely monitored with blood collection and symptom reporting, until three consecutive stool samples tested negative for ETEC (mean 6.9 days, range 5–9). Diarrhea was defined as one loose/liquid stool exceeding 300 g or ≥ 2 loose/liquid stools exceeding 200 g within any 48-h period within 120 h after the dose ingestion [12, 51]. Unless they fulfilled criteria for early antibiotic treatment, all volunteers were treated with ciprofloxacin 5 days after ETEC ingestion to clear the infection [12]. More details on design of the experimental infection study are described previously [12].

Whole blood collection and processing

We collected whole blood on seven timepoints (before infection, days 3, 5, 6, 7, 10, and 28) from each of the nine volunteers, giving a total of 63 specimens. After collection by venipuncture using EDTA Vacutainer tubes (BD Biosciences, San Jose, CA), the specimens were kept on ice until centrifugation at $2000 \times g$ for 10 min at 4°C. Following removal of the top layer of plasma, we carefully aspirated buffy coats and immediately fixed them using stable-lyse/stable-store V2 reagents (Smart Tube Inc, San Carlos, CA) according to the manufacturer's instructions and stored aliquots at -80°C .

We developed a panel consisting of seven metal-conjugated CD45-antibodies for barcoding and 34 metal-conjugated antibodies targeting cell surface markers (Supporting Information Table S1). The antibodies were titrated according to established principles [52]. Chemokine receptor antibodies CXCR3, CCR4, and CCR6 were omitted due to poor performance with the used fixation method [53]. Details on sample thawing, PBMC preparation, staining, acquisition, and normalization are given in Supporting Information.

Unsupervised and supervised clustering

The normalized cell data were initially clustered by the unsupervised algorithm *X-shift* on the program platform Vortex [54]. The computations were performed on virtual instances on Norwegian Research and Education Cloud (NREC), provided by University of Bergen and University of Oslo. The channels used for clustering by *X-shift* focused on phenotypic markers (Supporting Information Table S1). The markers CD185 (CXCR5), CD154 (CD40-L), and CTLA-4 (CD152) were not included in the final analysis due to suboptimal signals obtained during experiments. *X-shift* identified 163 clusters at $k = 500$. Twenty-four clusters containing small monocyte populations, very small and inconsistent T-cell populations, or artifactual populations were discarded. The remaining 139 clusters were manually merged into a total of 33 cell populations based on their phenotypical marker similarity, which corresponded to established marker profiles of classic lymphocyte populations (Table 1).

Statistical analysis

To examine population dynamics, we calculated fold changes of each cell population's proportion from baseline (day 0 before the dose ingestion) to follow-up timepoints within the diarrhea and nondiarrhea groups. Statistical significance was evaluated using Wilcoxon signed rank tests. For the functional markers, we used the same Wilcoxon signed rank tests for differences in arcsinh-transformed values of 80th percentile cut-offs (60th percentile for $\beta 7$ and 50th percentile for CD38) of the signal intensity for the functional markers, using the Python package *statsmodels* (SC-Introduction) [55]. We used Mann–Whitney *U* test to investigate differences in cell population proportions between the groups at a given timepoint, with the Python package *statsmodels*. Heatmaps and boxplots were created using the Python packages *seaborn* and *bioinfokit* [56, 57]. Fold changes used in the analysis are the medians of fold changes for each volunteer per timepoint. Spearman correlation tests were used to evaluate correlation in population proportion changes between two cell populations. Due to the exploratory nature of this study, *p*-values were not adjusted for multiplicity, and only diarrhea group with six volunteers were subjected to the statistical testing. Graphical abstract was created with *BioRender*.

Acknowledgements: We sincerely thank the volunteers who allowed us to perform this study, and the initiator of human experimental ETEC infection studies at UiB, Halvor Sommerfelt. We thank the Department of Medicine at Haukeland University Hospital for hosting the study, and especially personnel at the Department for Infectious Diseases Ward 5V, for all assistance during the in-patient period of the study. The mass cytometry

experiments were performed at the Flow Cytometry Core Facility, Department of Clinical Science, University of Bergen. We are grateful for the efforts of Brith Bergum in providing invaluable technical assistance throughout the study. We also thank Reidun Kristin Kopperud for teaching conjugation of antibodies, and Sturla Magnus Grøndal for assistance in CyTOF data acquisition. We thank Nello Blaser for teaching us basic concepts in unsupervised clustering and mathematical/statistical background as a thread of machine learning. This work was partly supported by the University of Bergen, Gades Legat and the Research Council of Norway through the Global Health and Vaccination Program (GLOBVAC) (<https://www.forskingsradet.no/en/>), project number 234364, and the FORNY program, project number 260686, with primary recipients as Kurt Hanevik and Hans Steinsland. The Helios Mass Cytometer was funded by Bergen Research Foundation.

Conflict of interests: All authors declare no commercial or financial conflict of interest.

Author contributions: K.H. and H.S. were associated with study conceptualization and funding. K.H., S.T.S., S.R., S.E.G., F.Z., J.S., and S.K.C. were associated with methodology development. K.H., S.R., S.T.S., and S.E.G. was involved in data acquisition and interpretation. S.R. did data analysis and visualization and wrote the original draft of the manuscript assisted by S.T.S. and K.H. H.S., S.E.G., F.Z., J.S., and S.K.C. reviewed and edited the final manuscript. K.H. designed and supervised the study.

Ethics statement: Informed written consent was obtained from all volunteers participating in the study. The study was approved by the Regional Committee for Medical and Health Research Ethics, Health Region West (Project ID: 2014-826), and registered at ClinicalTrials.gov (Project ID: NCT02870751).

Data availability statement: The data that support the findings of this study are available from the corresponding author upon reasonable request.

Peer review: The peer review history for this article is available at <https://publons.com/publon/10.1002/eji.202250254>

References

- 1 Khalil, I. A., Troeger, C., Blacker, B. F., Rao, P. C., Brown, A., Atherly, D. E., Brewer, T. et al., Morbidity and mortality due to shigella and enterotoxigenic *Escherichia coli* diarrhoea: The Global Burden of Disease Study 1990–2016. *Lancet Infect. Dis.* 2018. 18: 1229–1240.
- 2 Walker, R. I., An assessment of enterotoxigenic *Escherichia coli* and *Shigella* vaccine candidates for infants and children. *Vaccine* 2015. 33: 954–965.
- 3 Fleckenstein, J. M., Hardwidge, P. R., Munson, G. P., Rasko, D. A., Sommerfelt, H. and Steinsland, H., Molecular mechanisms of enterotoxigenic *Escherichia coli* infection. *Microbes Infect.* 2010. 12: 89–98.

- 4 Mani, S., Toapanta, F. R., McArthur, M. A., Qadri, F., Svennerholm, A. M., Devriendt, B., Phalipon, A. et al., Role of antigen specific T and B cells in systemic and mucosal immune responses in ETEC and Shigella infections, and their potential to serve as correlates of protection in vaccine development. *Vaccine* 2019. 37: 4787–4793.
- 5 Nielsen, M. M. and Witherden, D. A., Havran, W.L., $\gamma\delta$ T cells in homeostasis and host defence of epithelial barrier tissues. *Nat. Rev. Immunol.* 2017. 17: 733–745.
- 6 Wong, E. B., Ndung'u, T. and Kasprovicz, V. O., The role of mucosal-associated invariant T cells in infectious diseases. *Immunology* 2017. 150: 45–54.
- 7 Kolls, J. K. and Khader, S. A., The role of Th17 cytokines in primary mucosal immunity. *Cytokine Growth Factor Rev.* 2010. 21: 443–448.
- 8 Hinks, T. S. C. and Zhang, X.-W., MAIT Cell activation and functions. *Front. Immunol.* 2020. 11. <https://doi.org/10.3389/fimmu.2020.01014>
- 9 Leach, S., Clements, J. D., Kaim, J. and Lundgren, A., The adjuvant double mutant *Escherichia coli* heat labile toxin enhances IL-17A production in human T cells specific for bacterial vaccine antigens. *PLoS One* 2012. 7: e51718.
- 10 Frederick, D. R., Goggins, J. A., Sabbagh, L. M., Freytag, L. C., Clements, J. D. and McLachlan, J. B., Adjuvant selection regulates gut migration and phenotypic diversity of antigen-specific CD4(+) T cells following parenteral immunization. *Mucosal Immunol.* 2018. 11: 549–561.
- 11 Wennerås, C., Svennerholm, A. M. and Czerkinsky, C., Vaccine-specific T cells in human peripheral blood after oral immunization with an inactivated enterotoxigenic *Escherichia coli* vaccine. *Infect. Immun.* 1994. 62: 874–879.
- 12 Sakkestad, S. T., Steinsland, H., Skrede, S., Lillebø, K., Skutlaberg, D. H., Guttormsen, A. B., Zavialov, A. et al., A new human challenge model for testing heat-stable toxin-based vaccine candidates for enterotoxigenic *Escherichia coli* diarrhea—Dose optimization, clinical outcomes, and CD4+ T cell responses. *PLoS Negl. Trop. Dis.* 2019. 13: e0007823.
- 13 McArthur, M. A., Chen, W. H., Magder, L., Levine, M. M. and Sztein, M. B., Impact of CD4+ T cell responses on clinical outcome following oral administration of wild-type enterotoxigenic *Escherichia coli* in humans. *PLoS Negl. Trop. Dis.* 2017. 11: e0005291.
- 14 Cárdeno, A., Magnusson, M. K., Quiding-Järbrink, M. and Lundgren, A., Activated T follicular helper-like cells are released into blood after oral vaccination and correlate with vaccine specific mucosal B-cell memory. *Sci. Rep.* 2018. 8: 2729.
- 15 Aggarwal, S., Ghilardi, N., Xie, M. H., de Sauvage, F. J. and Gurney, A. L., Interleukin-23 promotes a distinct CD4 T cell activation state characterized by the production of interleukin-17. *J. Biol. Chem.* 2003. 278: 1910–1914.
- 16 Langrish, C. L., Chen, Y., Blumenschein, W. M., Mattson, J., Basham, B., Sedgwick, J. D., McClanahan, T. et al., IL-23 drives a pathogenic T cell population that induces autoimmune inflammation. *J. Exp. Med.* 2005. 201: 233–240.
- 17 Annunziato, F., Cosmi, L., Santarlasci, V., Maggi, L., Liotta, F., Mazzinghi, B., Parente, E. et al., Phenotypic and functional features of human Th17 cells. *J. Exp. Med.* 2007. 204: 1849–1861.
- 18 Sallusto, F., Zielinski, C. E. and Lanzavecchia, A., Human Th17 subsets. *Eur. J. Immunol.* 2012. 42: 2215–2220.
- 19 Ornatsky, O., Bandura, D., Baranov, V., Nitz, M., Winnik, M. A. and Tanner, S., Highly multiparametric analysis by mass cytometry. *J. Immunol. Methods* 2010. 361: 1–20.
- 20 Napolitani, G., Kurupati, P., Teng, K. W. W., Gibani, M. M., Rei, M., Alicino, A., Preciado-Llanes, L. et al., Clonal analysis of Salmonella-specific effector T cells reveals serovar-specific and cross-reactive T cell responses. *Nat. Immunol.* 2018. 19: 742–754. <https://doi.org/10.1038/s41590-018-0133-z>
- 21 McArthur, M. A., Fresnay, S., Magder, L. S., Darton, T. C., Jones, C., Waddington, C. S., Blohmke, C. J. et al., Activation of *Salmonella* Typhi-specific regulatory T cells in typhoid disease in a wild-type *S. Typhi* challenge model. *PLoS Pathog.* 2015. 11: e1004914.
- 22 Vedøy, O. B., Steinsland, H., Sakkestad, S. T., Sommerfelt, H. and Hanevik, K., Strong association between diarrhea and concentration of enterotoxigenic *Escherichia coli* strain TW10722 in stools of experimentally infected volunteers. *Pathogens* 2023. 12: 283. <https://doi.org/10.3390/pathogens12020283>
- 23 Sallusto, F., Lenig, D., Förster, R., Lipp, M. and Lanzavecchia, A., Two subsets of memory T lymphocytes with distinct homing potentials and effector functions. *Nature* 1999. 401: 708–712.
- 24 Hamann, D., Baars, P. A., Rep, M. H., Hooibrink, B., Kerkhof-Garde, S. R., Klein, M. R. and van Lier, R. A., Phenotypic and functional separation of memory and effector human CD8+ T cells. *J. Exp. Med.* 1997. 186: 1407–1418.
- 25 Cosmi, L., De Palma, R., Santarlasci, V., Maggi, L., Capone, M., Frosali, F., Rodolico, G. et al., Human interleukin 17-producing cells originate from a CD161+CD4+ T cell precursor. *J. Exp. Med.* 2008. 205: 1903–1916.
- 26 Bai, A. and Robson, S., Beyond ecto-nucleotidase: CD39 defines human Th17 cells with CD161. *Purinergic Signal* 2015. 11: 317–319.
- 27 Maroof, A., Beattie, L., Zubairi, S., Svensson, M., Stager, S. and Kaye, P. M., Posttranscriptional regulation of IL10 gene expression allows natural killer cells to express immunoregulatory function. *Immunity* 2008. 29: 295–305.
- 28 Gao, Y. and Williams, A. P., Role of innate T cells in anti-bacterial immunity. *Front. Immunol.* 2015. 6. <https://doi.org/10.3389/fimmu.2015.00302>
- 29 Feurle, J., Espinosa, E., Eckstein, S., Pont, F., Kunzmann, V., Fournié, J. J., Herderich, M. et al., *Escherichia coli* produces phosphoantigens activating human gamma delta T cells. *J. Biol. Chem.* 2002. 277: 148–154.
- 30 Barisa, M., Kramer, A. M., Majani, Y., Moulding, D., Saraiva, L., Bajaj-Elliott, M., Anderson, J. et al., *E. coli* promotes human $\gamma\delta$ T cell transition from cytokine-producing bactericidal effectors to professional phagocytic killers in a TCR-dependent manner. *Sci. Rep.* 2017. 7: 2805.
- 31 Schaut, R. G., Boggiatto, P. M., Loving, C. L. and Sharma, V. K., Cellular and mucosal immune responses following vaccination with inactivated mutant of *Escherichia coli* O157:H7. *Sci. Rep.* 2019. 9: 6401.
- 32 Eller, M. A., Lal, K. G., Kim, D., Vasan, S., Gramzinski, R. A. and Maciel, M., Peripheral blood MAIT cell response to enterotoxigenic *E. coli* strains H10407 and B7A after controlled human infection models (CHIMs). *J. Immunol.* 2020. 204(1): 148.25.
- 33 Le Bourhis, L., Martin, E., Péguillet, I., Guihot, A., Froux, N., Coré, M., Lévy, E. et al., Antimicrobial activity of mucosal-associated invariant T cells. *Nat. Immunol.* 2010. 11: 701–708.
- 34 Salerno-Goncalves, R., Luo, D., Fresnay, S., Magder, L., Darton, T. C., Jones, C., Waddington, C. S. et al., Challenge of humans with wild-type *Salmonella enterica* serovar Typhi elicits changes in the activation and homing characteristics of mucosal-associated invariant T cells. *Front. Immunol.* 2017. 8: 398.
- 35 Alves, N. L., van Leeuwen, E. M., Remmerswaal, E. B., Vrisekoop, N., Teselaar, K., Roosnek, E., ten Berge, I. J. M. et al., A new subset of human naive CD8+ T cells defined by low expression of IL-7R alpha. *J. Immunol.* 2007. 179: 221–228.
- 36 Sehrawat, S. and Rouse, B. T., Interplay of regulatory T cell and Th17 cells during infectious diseases in humans and animals. *Front. Immunol.* 2017. 8: 341.

- 37 Kuchta, A., Rahman, T., Sennott, E. L., Bhuyian, T. R., Uddin, T., Rashu, R., Chowdhury, F. et al., *Vibrio cholerae* O1 infection induces proinflammatory CD4⁺ T-cell responses in blood and intestinal mucosa of infected humans. *Clin. Vaccine Immunol.* 2011. **18**: 1371–1377.
- 38 Atarashi, K., Tanoue, T., Ando, M., Kamada, N., Nagano, Y., Narushima, S., Suda, W. et al., Th17 cell induction by adhesion of microbes to intestinal epithelial cells. *Cell* 2015. **163**: 367–380.
- 39 Tesmer, L. A., Lundy, S. K., Sarkar, S. and Fox, D. A., Th17 cells in human disease. *Immunol. Rev.* 2008. **223**: 87–113.
- 40 Ren, W., Yin, J., Xiao, H., Chen, S., Liu, G., Tan, B., Li, N. et al., Intestinal microbiota-derived GABA mediates interleukin-17 expression during enterotoxigenic *Escherichia coli* infection. *Front. Immunol.* 2017. **7**: 685.
- 41 Luo, Y., Van Nguyen, U., Fe Rodriguez, de la P. Y., Devriendt, B. and Cox, E., F4+ ETEC infection and oral immunization with F4 fimbriae elicits an IL-17-dominated immune response. *Vet. Res.* 2015. **46**: 121.
- 42 Belkaid, Y. and Rouse, B. T., Natural regulatory T cells in infectious disease. *Nat. Immunol.* 2005. **6**: 353–360.
- 43 Chang, H. S. and Sack, D. A., Development of a novel in vitro assay (ALS assay) for evaluation of vaccine-induced antibody secretion from circulating mucosal lymphocytes. *Clin. Diagn. Lab. Immunol.* 2001. **8**: 482–488.
- 44 Crome, S. Q., Wang, A. Y., Kang, C. Y. and Levings, M. K., The role of retinoic acid-related orphan receptor variant 2 and IL-17 in the development and function of human CD4⁺ T cells. *Eur. J. Immunol.* 2009. **39**: 1480–1493.
- 45 Todnem Sakkestad, S., Steinsland, H., Skrede, S., Kleppa, E., Lillebø, K., Sævik, M., Søyland, H. et al., Experimental infection of human volunteers with the heat-stable enterotoxin-producing enterotoxigenic *Escherichia coli* strain TW11681. *Pathogens* 2019. **8**: 84.
- 46 Levine, M. M., Nalin, D. R., Hoover, D. L., Bergquist, E. J., Hornick, R. B. and Young, C. R., Immunity to enterotoxigenic *Escherichia coli*. *Infect. Immun.* 1979. **23**: 729–736.
- 47 Braudeau, C., Salabert-Le Guen, N., Chevreuil, J., Rimbart, M., Martin, J. C. and Josien, R., An easy and reliable whole blood freezing method for flow cytometry immuno-phenotyping and functional analyses. *Cytometry B Clin. Cytom.* 2021. **100**: 652–665.
- 48 Langweiler, M., Immunophenotyping using dried and lyophilized reagents. *Methods Mol. Biol.* 2019. **2032**: 69–79.
- 49 Moris, P., Bellanger, A., Ofori-Anyinam, O., Jongert, E., Yarzabal Rodriguez, J. P. and Janssens, M., Whole blood can be used as an alternative to isolated peripheral blood mononuclear cells to measure in vitro specific T-cell responses in human samples. *J. Immunol. Methods* 2021. **492**: 112940.
- 50 Steinsland, H., Lacher, D. W., Sommerfelt, H. and Whittam, T. S., Ancestral lineages of human enterotoxigenic *Escherichia coli*. *J. Clin. Microbiol.* 2010. **48**: 2916–2924.
- 51 Harro, C., Chakraborty, S., Feller, A., DeNearing, B., Cage, A., Ram, M., Lundgren, A. et al., Refinement of a human challenge model for evaluation of enterotoxigenic *Escherichia coli* vaccines. *Clin. Vaccine Immunol.* 2011. **18**: 1719–1727.
- 52 Gullaksen, S. E., Bader, L., Hellesøy, M., Sulen, A., Fagerholt, O. H. E., Engen, C. B., Skavland, J. et al., Titrating complex mass cytometry panels. *Cytometry A* 2019. **95**: 792–796.
- 53 Sakkestad, S. T., Skavland, J. and Hanevik, K., Whole blood preservation methods alter chemokine receptor detection in mass cytometry experiments. *J. Immunol. Methods* 2020. **476**: 112673.
- 54 Samusik, N., Good, Z., Spitzer, M. H., Davis, K. L. and Nolan, G. P., Automated mapping of phenotype space with single-cell data. *Nat. Methods* 2016. **13**: 493–496.
- 55 Seabold, S. and Perktold, J., Statsmodels: econometric and statistical modeling with python. *Proceedings of the 9th Python in Science Conference*, 2010.
- 56 Waskom, M., seaborn: statistical data visualization. *J. Open Source Software* 2021. **6**: 3021.
- 57 Huang, Y., Wang, J. Y., Wei, X. M. and Hu, B., Bioinfo-Kit: a sharing software tool for bioinformatics. *Appl. Mech. Mater.* 2014. **472**: 466–469.

Abbreviations: ETEC: enterotoxigenic *Escherichia coli* · MAIT: mucosal associated invariant T · SC: supplementary charts · T_{EM}: effector memory T · T_{CM}: central memory T · CS: coli surface antigens

Full correspondence: Prof. Kurt Hanevik, Department of Clinical Science, Faculty of Medicine, University of Bergen, Bergen, Norway
e-mail: kurt.hanevik@uib.no

Received: 3/11/2022
Revised: 11/3/2023
Accepted: 24/4/2023
Accepted article online: 27/4/2023